Kinetic and Mutagenic Studies of the Role of the Active Site Residues Asp-50 and Glu-327 of *Escherichia coli* Glutamine Synthetase†

Murtaza Alibhai‡ and Joseph J. Villafranca*

Department of Chemistry, The Pennsylvania State University, University Park, Pennsylvania 16802

Received August 3, 1993; Revised Manuscript Received September 30, 1993®

ABSTRACT: The role of Asp-50 and Glu-327 of *Escherichia coli* glutamine synthetase in catalysis and substrate binding has been interrogated by construction of site-directed mutants at these positions. Steady-state and rapid-quench kinetic methods were used to elucidate contributions of Asp-50 and Glu-327 to the K_m values of all three substrates, ATP, glutamate, and NH_4^+, as well as to the enzymatic k_{cat} value. Kinetic constants were obtained for the D50A enzyme using both Mg^{2+} and Mn^{2+} as activating metal ions; the data reveal that Asp-50 has a significant role in both substrate binding and catalysis as reflected by the increases in the K_m values for NH_4^+ and the destabilization of both the ground state and the transition state for phosphoryl transfer. The D50E mutant was found to have activity with Mn^{2+} but very low activity with Mg^{2+}, the physiologically important metal ion. The k_{cat}/K_m values for all three substrates were substantially altered by changing Asp to Glu. The steady-state results for the E327A mutant indicate a decreased k_{cat}/K_m value for NH_4^+ compared to that of the wild-type enzyme. The E327A-Mg^{2+} enzyme destabilizes the ground state of the ternary complex (E–ATP–Glu-NH_4^+) and the transition state for phosphoryl transfer while the E327A-Mn^{2+}-enzyme provides greater stabilization for the ATP and glutamate complexes but destabilizes phosphoryl transfer steps in the ternary complex. Overall, these results suggest that Asp-50 is likely involved in binding NH_4^+ and may also play a role in catalyzing deprotonation of NH_4^+ to form NH_3. Glu-327 participates in lowering the free energy of the transition state involved in formation of the positively charged tetrahedral adduct resulting from the condensation of γ-glutamyl phosphate and NH_3.

Glutamine synthetase (GS)[1] is a key enzyme in nitrogen metabolism. It catalyzes the biosynthesis of L-glutamine from L-glutamate, ATP, and NH_4^+ (eq 1).

$$\text{L-glutamate} + \text{ATP} + NH_4^+ \xrightarrow{GS,M^{2+}} \text{L-glutamine} + \text{ADP} + P_i \quad (1)$$

Glutamine synthetase from *Escherichia coli* consists of 12 identical subunits with each subunit having a molecular weight of ca. 52 000 (Stadman & Ginsburg, 1974; Colombo & Villafranca, 1986). The X-ray crystal structure of the enzyme from *Salmonella typhimurium* reported at 3.5-Å resolution demonstrates that the subunits are arranged in two hexamers stacked face to face; the side-to-side interface of a pair of subunits constitutes an active site containing two Mn^{2+} ions (Almassy et al., 1986; Yamashita et al., 1989). The *E. coli* and *S. typhimurium* GS atomic models are now available to 2.8-Å resolution (Liaw, 1992; Liaw et al., 1993), and these two enzymes are 98% identical at the nucleotide level, differing at only 10 amino acid residues per subunit (Janson et al., 1986; Wray & Fisher, 1988). Hence, the structures of the two enzymes are assumed to be identical.

The two divalent metal ions in the active site are distinguished by their dissociation constants (Denton & Ginsburg, 1969; Villafranca et al., 1985). Saturation of the high-affinity site, n_1, in each subunit by Mn^{2+} or Mg^{2+} induces a conformational change converting the enzyme from a catalytically inactive, *relaxed* form to a catalytically active *taut* conformation (Shapiro & Ginsburg, 1968; Hunt & Ginsburg, 1972). The metal ion at the n_1 site also plays a catalytic role in the binding glutamate (Hunt & Ginsburg, 1980; Villafranca et al., 1976a,b). The second divalent metal ion, n_2, in each subunit is thought to be involved in the binding of the substrate, ATP (Hunt et al., 1975).

Amino acid sequence comparisons of GS from prokaryotes (Wray & Fisher, 1988) and X-ray crystallographic studies of the enzyme indicated that Asp-50 and Glu-327 were highly conserved residues, present in the active site. Upon examination of the structural data for the GS–methionine sulfoximine complex (mimic of the tetrahedral adduct) (Liaw & Eisenberg, 1994), it was observed that Asp-50 and Glu-327 formed a negatively charged "pocket" approximately 7 Å from the n_1 metal ion site. This arrangement of amino acids as a negatively charged pocket led to the speculation that NH_4^+ may bind in this location and that site-directed mutagenesis studies would be useful to test this hypothesis. Previous kinetic studies (Colanduoni et al., 1987) indicated that NH_3 is the active species in the biosynthetic reaction, and, hence, NH_4^+ must be deprotonated in order to act as a nucelophile. Therefore, either Asp-50 or Glu-327 might be the base responsible for the deprotonation of NH_4^+, and these residues may also serve as the specificity "pocket" for this molecule. Glutamine synthetase is highly selective for NH_4^+ over H_2O and exclusively catalyzes glutamine formation instead of aberrant hydrolysis of the highly reactive γ-glutamyl phosphate formed as an intermediate during the reaction cycle (Clark & Villafranca, 1985). Thus, the specificity for NH_4^+

† This research was supported by National Institutes of Health Grant GM23529.

* To whom correspondence should be addressed at Bristol-Myers Squibb, Pharmaceutical Research Institute, P.O. Box 4000, Princeton, NJ 08543-4000.

‡ Current address: Genentech 460 Point San Bruno Blvd., South San Francisco, CA 94080.

® Abstract published in *Advance ACS Abstracts,* December 1, 1993.

[1] Abbreviations: GS, Glutamine synthetase; PCR, polymerase chain reaction; EDTA, ethylenediaminetetraacetic acid; PEP, phosphoenolpyruvate; HEPES, *N*-(2-hydroxyethyl)piperazine-*N'*-(2-ethanesulfonic acid); PIPES, piperazine-*N,N'*-bis(2-ethanesulfonic acid).

0006-2960/94/0433-682$04.50/0

binding by glutamine synthetase is well established. It is reasonable to presume that the positively charged adduct formed after NH_3 attacks γ-glutamyl phosphate would also be stabilized in this negatively charged pocket.

In this paper, steady-state and pre-steady-state kinetic techniques were used to assess the notion that Asp-50 and Glu-327 are involved in substrate binding and/or catalysis. The X-ray structure of GS at 2.8 Å in complex with substrates and intermediate analogs provides data to support the involvement of both Asp-50 and Glu-327 in binding and catalysis (Liaw & Eisenberg, 1994).

EXPERIMENTAL PROCEDURES

Materials

Amplitaq DNA polymerase was purchased from Perkin-Elmer Cetus. All restriction enzymes were purchased from New England Biolabs. Oligonucleotides were purchased from Bio-Synthesis and purified using PAGE and HPLC. [γ-^{32}P]-ATP(20–50 Ci/mmol) was obtained from New England Nuclear and was purified using HPLC on a Pharmacia Mono Q HR 5/5 column (Lewis & Villafranca, 1989). All other chemicals were obtained from Sigma.

Methods

Site-Directed Mutagenesis. A single round of PCR was used for the construction of D50A and D50E mutants. A primer (36-mer) at the 5′ end of the *glnA* gene in conjuction with another primer (27-mer) at the 3′ end of the *glnA* gene was used for the PCR. The primer at the 3′ end had the desired sequence change and also incorporated an *Asu*II site. Typically, 25 cycles of PCR were performed, and the amplified segment was gel purified. The restriction enzymes *Bgl*II and *Asu*II were used to subclone the fragments containing the mutation into pgln35, and the mutant plasmid was transformed into the YMC21E strain of *E. coli* for the expression of the mutant enzymes. Plasmid pgln35 contains the *glnALG* operon cloned into pBR322 (Chen et al., 1982). GS expressed in YMC21E is fully unadenylylated due to the deletion of *glnE* gene, which encodes ATP:glutamine synthetase adenylyltransferase, the enzyme which catalyzes the adenylylation of GS. Also, strain YMC21E contains a deletion of the *glnA* gene in the chromosome, which codes for GS, and hence any DNA expressed in YMC21E was not contaminated with the WT enzyme. A limitation of PCR-based methods is the rate of nucleotide misincorporation during PCR, and, hence, the entire *glnA* gene for each mutant was sequenced to verify that only the desired mutation was introduced.

Enzyme Purification. Unadenylylated glutamine synthetase was isolated from *E. coli* YMC21E/pgln35 grown in minimal media containing 1 mM $MnCl_2$. The $MnCl_2$ is added to inhibit oxidation of GS (Roseman & Levine, 1987). The enzyme was purified according to the procedure of Roseman and Levine (1987). The purification included a streptomycin sulfate precipitation step, zinc sulfate cut, acetone precipitation, and an ammonium sulfate precipitation step. After purification, the enzyme was stored in 10 mM imidazole (pH 7.2), 100 mM KCl, and 1 mM $MnCl_2$ at 4 °C.

Wild-type enzyme concentrations were determined spectrophotometrically (Stadtman & Ginsburg, 1974), and the concentrations of the mutant enzymes were determined using the enhanced protocol of the Pierce BCA Protein Assay Reagent kit. The Mn^{2+} ions in glutamine synthetase were replaced with Mg^{2+} ions by dialyzing the enzyme in Mn^{2+}-containing buffer into 50 mM HEPES (pH 7.5), 100 mM KCl, and 5 mM EDTA for 12 h followed by dialysis against 50 mM HEPES (pH 7.5), 100 mM KCl, and 25 mM $MgCl_2$ for 20 h. The enzyme with Mg^{2+} was found to be stable for 3 weeks at 4 °C.

Steady-State Kinetics. The biosynthetic activity of GS using Mn^{2+} or Mg^{2+} as the activating metal ion was measured spectrophotometrically using the pyruvate kinase–lactate dehydrogenase coupling system (Ginsburg et al., 1970). All experiments were done at 25 °C using a Cary 2200 UV/vis spectrophotometer. For the Mn^{2+}-activated assay, the assay solution contained 50 mM PIPES (pH 6.5), 100 mM KCl, 1 mM PEP, 150 μg NADH, 35 μg/mL pyruvate kinase, and 35 μg/mL L-lactate dehydrogenase. For reactions with Mg^{2+} as the activating metal ion, 50 mM HEPES (pH 7.5) was used instead of PIPES. The K_m values for ATP, glutamate, and ammonia were determined by varying one of the substrates while keeping the others at saturating concentrations (5–10 times the K_m value). The oxidation of NADH was monitored at 340 nm, and the initial rates were obtained using SPECTRA CALC.

Rapid-Quench Experiments. Rapid-quench studies of the biosynthetic reaction were conducted at 10 °C using an instrument from Kintek (Johnson, 1986). A solution containing enzyme (0.039 mL) was rapidly mixed with one containing all substrates (0.042 mL) including 0.25 mM PEP and 0.01 mg/mL pyruvate kinase and trace amounts of [γ-^{32}P]-ATP (6500 cpm/nmol of ATP). Pyruvate kinase and PEP were added to prevent the accumulation of ADP, which is a potent product inhibitor.

Experiments were conducted at 10 °C to allow accurate measurements of the burst rates. Reactions were quenched with 199 μL of 0.6 N HCl at different times, and the resulting solution was immediately neutralized with 45 μL of 1 M Tris and 4 M KOH solution. A 1-mL aliquot of pyrophosphate buffer (65 mM H_3PO_4 and 10 mM $Na_4P_2O_7$) was added to each reaction sample, and 200 μL of the resulting solution was removed and counted for total radioactivity. The remaining solution was placed on an activated charcoal column (Johnson, 1986) and eluted with 15 mL of pyrophosphate buffer and counted.

All experiments with Mn^{2+} as the activating metal ion were carried out at pH 6.5 and contained 60 μM enzyme subunits, 100 mM PIPES, 100 mM KCl, and 8 mM $MnCl_2$ in the final reaction mixture. Experiments with Mg^{2+} as the activating metal ion were carried out at pH 7.5 and contained 60 μM enzyme subunits, 50 mM HEPES, 100 mM KCl, 25 mM $MgCl_2$ for the wild-type enzyme, and 75 mM $MgCl_2$ for the E327A mutant enzyme. All substrates were present at 5–10 times the K_m value except in the case of D50E-Mn^{2+}, WT-Mg^{2+}, and E327A-Mg^{2+} enzymes where ATP was added at 3 times the K_m value. Saturating concentration of ATP could not be used because the K_m value for ATP is too large.

Data Analysis. Steady-state kinetic data were analyzed using KINETASYST (IntelliKinetics, Princeton, NJ). Rapid-quench data were fit to eq 2for single-exponential "bursts"

$$P_i/E = A(1 - e^{-\lambda t}) + k_{ss}t \qquad (2)$$

where P_i is the concentration of radioactive inorganic phosphate, E is enzyme subunit concentration, A is the transient burst amplitude, λ is the transient rate constant, k_{ss} is the steady-state rate constant, and t is the time.

Calculation of Free Energy Levels. The energy level, G, of each state of the enzyme was calculated using the rate constants obtained from rapid-quench studies and the K_m

Table 1: Steady-State Kinetic Parameters[a]

enzyme	metal	K_m^{Glu} (mM)	K_m^{ATP} (μM)	$K_m^{NH_4^+}$ (mM)	k_{cat} (s^{-1})
WT	Mn^{2+}	0.05 ± 0.01	0.6 ± 0.1	0.10 ± 0.02	2.0 ± 0.2
D50A	Mn^{2+}	0.20 ± 0.02	3.6 ± 0.3	44 ± 4	3.0 ± 0.2
D50E	Mn^{2+}	5.4 ± 0.4	310 ± 30	1.20 ± 0.04	10.0 ± 0.4
E327A	Mn^{2+}	0.04 ± 0.01	1.0 ± 0.1	2.5 ± 0.3	1.0 ± 0.1
WT	Mg^{2+}	5.5 ± 0.6	400 ± 40	0.10 ± 0.01	50 ± 4
D50A	Mg^{2+}	8 ± 1	600 ± 30	54 ± 5	29.0 ± 0.2
D50E	Mg^{2+}	54 ± 7	600 ± 40	0.10 ± 0.01	0.10 ± 0.02
E327A	Mg^{2+}	2.0 ± 0.1	160 ± 10	13 ± 1	25 ± 2

[a] All measurements were conducted at 25 °C as described under Methods.

Table 2: Specificity Constants for the Substrates[a]

enzyme	metal	k_{cat}/K_m^{Glu} (s^{-1} mM^{-1})	k_{cat}/K_m^{ATP} (s^{-1} μM^{-1})	$k_{cat}/K_m^{NH_4^+}$ (s^{-1} mM^{-1})
WT	Mn^{2+}	40	3.3	20
D50A	Mn^{2+}	15	0.8	0.1
D50E	Mn^{2+}	1.9	0.03	8.3
E327A	Mn^{2+}	25	1.0	0.4
WT	Mg^{2+}	9.1	0.1	500
D50A	Mg^{2+}	3.6	0.05	0.5
D50E	Mg^{2+}	0.002	0.0002	1.0
E327A	Mg^{2+}	12.5	0.2	2.0

[a] All measurements were conducted at 25 °C as described under Methods.

values for each substrate. A standard state of 1 M was used for all substrates (Wells & Fersht, 1986).

RESULTS AND DISCUSSION

Steady-State Kinetics. Site-directed mutagenesis has been applied to study the roles of Asp-50 and Glu-327 in the catalytic mechanism of *E. coli* glutamine synthetase. Three mutants, D50A, D50E, and E327A, were constructed for this purpose. The steady-state kinetic parameters for wild-type and mutant forms of GS are summarized in Table 1. All assays were done at pH 6.5 or 7.5 for Mn^{2+} or Mg^{2+}, respectively, as the activating metal ion. With Mn^{2+}, the D50A enzyme is more active than WT GS while the D50E enzyme is 8-fold more active. With Mg^{2+}, the D50A mutant GS shows a slight decrease in activity while the D50E mutant enzyme shows a significant loss in activity (500-fold). The K_m values for ammonia are larger for all mutant enzymes with Mn^{2+}, with the largest increase found for the D50A mutant. With Mg^{2+} as the activating metal ion, there is no change in the K_m value for ammonia for D50E mutant GS, but the D50A and E327A mutants have significantly higher K_m values. Table 2 shows the specificity parameters for all three substrates for both WT and mutant forms of GS. With both Mg^{2+} and Mn^{2+}, all mutant forms of GS have lower specificity constants for ammonia, while the specificity constants for glutamate and ATP are altered greatly only with the D50E mutant.

Rapid-Quench Experiments. Rapid-quench experiments were conducted to investigate the effect of mutation of Glu-327 and Asp-50 on individual rate steps in the catalytic mechanism. The kinetic parameters obtained from rapid-quench studies are summarized in Table 3. The time courses for the quench flow experiments with WT-Mn^{2+} and D50E-Mn^{2+} are shown in Figure 1. Reactions were examined for at least six, half-lives to observe the first enzyme turnover (Johnson, 1992). For experiments conducted with Mn^{2+} as the activating metal ion at pH 6.5, a burst of acid-labile phosphate followed by a slower steady-state phase was observed for the wild-type, D50A, and E327A enzymes, but no clear burst was observed for the D50E enzyme. Also, a slight burst

Table 3: Rapid-Quench Kinetic Parameters[a]

enzyme	metal	pH	λ	A	k_{ss} (s^{-1})
WT	Mn^{2+}	6.5	13 ● 3	0.5 ± 0.1	0.4 ± 0.1
D50A	Mn^{2+}	6.5	16 ± 2	0.40 ± 0.02	0.40 ± 0.02
D50E	Mn^{2+}	6.5	340 ± 230	0.03 ± 0.01	0.20 ± 0.01
E327A	Mn^{2+}	6.5	11 ± 1	0.30 ± 0.02	0.20 ± 0.02
WT	Mg^{2+}	7.5	33 ± 20	0.4 ± 0.1	4.0 ± 0.2
E327A	Mg^{2+}	7.5	190 ± 90	0.30 ± 0.03	3.0 ± 0.1

[a] All measurements were conducted at 10 °C as described under Methods.

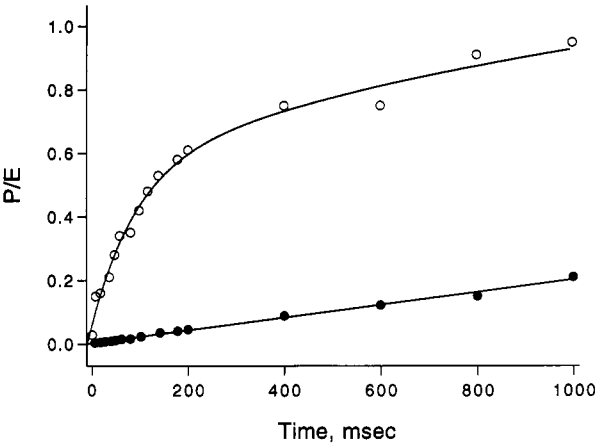

FIGURE 1: Time course of the Mn^{2+}-activated biosynthetic reaction catalyzed by wild-type and D50E mutant glutamine synthetases. All experiments were conducted at 10 °C and pH 6.5 (Experimental Procedures). Plots are the experimental data showing the formation of inorganic phosphate/enzyme (P/E) with time. D50E (●) and wild-type (○) enzyme. The solid line for wild-type enzyme is the fit to a single exponential.

Scheme 1

$$E + ATP \underset{k_{-1}}{\overset{k_1}{\rightleftharpoons}} E{\bullet}ATP + Glu \underset{k_{-2}}{\overset{k_2}{\rightleftharpoons}} E{\bullet}ATP{\bullet}Glu + NH_3 \underset{k_{-3}}{\overset{k_3}{\rightleftharpoons}}$$

$$E{\bullet}ATP{\bullet}Glu{\bullet}NH_3 \underset{k_{-4}}{\overset{k_4}{\rightleftharpoons}} E{\bullet}ADP{\bullet}Glu\text{–}P{\bullet}NH_3 \xrightarrow{k_5} E + P$$

Table 4: Kinetic Constants Calculated from Rapid-Quench Kinetic Data[a]

enzyme	metal	pH	k_4 (s^{-1})	k_{-4} (s^{-1})	k_5 (s^{-1})	k_4/k_{-4}
WT	Mn^{2+}	6.5	8.0	5.0	0.8	1.6
D50A	Mn^{2+}	6.5	7.0	8.0	0.8	0.9
D50E	Mn^{2+}	6.5	11	330	5.0	0.03
E327A	Mn^{2+}	6.5	3.0	7.0	0.7	0.4
WT	Mg^{2+}	7.5	18	7.4	7.5	2.6
E327A	Mg^{2+}	7.5	64	120	9.0	0.6

[a] All measurement were conducted at 10 °C as described under Methods.

was observed for the WT and E327A Mg^{2+}-activated enzymes. This suggests that, in the D50E-Mn^{2+} enzyme, a step preceding the chemical step is rate limiting or that the internal equilibrium (k_4/k_{-4}) may favor substrates (Johnson, 1992). The rate constants for individual steps in the biosynthetic reaction can be represented as shown in Scheme 1 (Meek et al., 1982; Abell & Villafranca, 1991).

Rate constants, k_4, k_{-4}, and k_5 can be obtained using the analysis employed by Meek et al. (1982) and are summarized in Table 4. As illustrated in Scheme 1, the ratio k_4/k_{-4} is the equilibrium constant for the transfer of the γ-phosphoryl group of ATP (K_{int}), and k_5 is the product release step.

Implications of the Kinetic Experiments. X-ray crystallographic studies indicated that Asp-50 and Glu-327 formed

a negatively charged "pocket" approximately 7 Å from the n_1 metal ion (Liaw & Eisenberg, 1994). These two residues are highly conserved among various prokaryotic species (Wray & Fisher, 1988) and might comprise the NH_4^+ ion binding site. We have previously shown that the catalytically important species is NH_3 in the biosynthetic reaction, and, hence, NH_4^+ must be deprotonated in order to act as a nucleophile (Colanduoni et al., 1987). Another potential catalytic role for Asp-50 or Glu-327 would be in the deprotonation of NH_4^+.

The steady-state results summarized in Table 1 indicate that the D50A-Mn^{2+} mutant has activity similar to that of the wild-type Mn^{2+}-enzyme, but the D50E-Mn^{2+} mutant has a higher k_{cat} value (5-fold). The higher activity of the D50E-Mn^{2+} enzyme is most likely due to the weaker binding of all the substrates, as reflected by the higher K_m values, as well as the weaker binding of products. With the Mn^{2+}-activated form of GS, product release is rate limiting, and any factor that leads to weaker binding of products will accelerate the overall velocity of the reaction (Abell & Villafranca, 1991). By contrast, the D50E-Mg^{2+} activated enzyme has very low activity. Proximity of the negatively charged carboxylate of glutamate 50 to the negatively charged substrates glutamate and ATP could produce the lowered k_{cat}/K_m values for these two substrates (Table 2). Indeed, the specificity constants for all three substrates are altered dramatically for this mutant. Alternatively, the change in catalytic activity exhibited by the two metal ions (Mn^{2+} and Mg^{2+}) for the D50E mutant might be due to altered binding of Mg^{2+} vs Mn^{2+} to the active site.

The D50A mutant exhibits the most drastic changes in K_m values for NH_4^+. The ca. 400–500-fold increase in $K_m(NH_4^+)$ was found with both Mn^{2+} and Mg^{2+} and contributes significantly to the decreased specificity constant for the ammonium ion (Table 2). The removal of the negative charge on the side chain with this mutant, and the consequent reduction in specificity constant, lead to the conclusion that Asp-50 plays a significant role in binding NH_4^+. These results also support an ancillary role for Asp-50 in the deprotonation of NH_4^+ for attack on the γ-glutamyl phosphate intermediate.

Glutamate 327 most likely plays a role in catalysis subsequent to formation of γ-glutamyl phosphate since the specificity constants for the substrates ATP and glutamate are not altered greatly by changing Glu-327 to Ala (Table 2). The largest kinetic changes found for the E327A mutant were not on catalytic activity but were in the K_m values for NH_4^+. Thus, the k_{cat}/K_m value for NH_4^+ is greatly affected, which suggests that Glu-327 plays a role in stabilizing the transition state for a reaction subsequent to NH_4^+ binding. This step could involve formation and/or breakdown of the tetrahedral intermediate which is zwitterionic. Glu-327 could stabilize the $-NH_3^+$ positive charge on this intermediate and perhaps assist in the deprotonation of the tetrahedral intermediate leading to formation of the product glutamine. The X-ray crystal structure of GS in complex with the transition state analog methionine sulfoximine (Liaw & Eisenberg, 1994) shows that movement of a protein loop consisting of residues 324–328 occurs when this analog is bound. This movement takes Glu-327 to within 2.6 Å of the location of the $-NH_3^+$ moiety of the tetrahedral intermediate consistent with its abovementioned role in catalysis.

Relative Free Energy Profiles for WT and Mutant GS. The free energy profiles in Figures 2 and 3 are based on all the kinetic data and show the effect of the mutations on the binding energies of the substrates and the stabilization of the

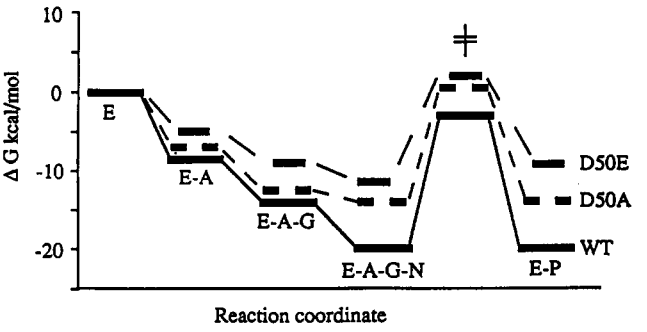

FIGURE 2: Free energy profile for the wild-type, D50A, and D50E Mn^{2+}-activated enzymes. E–A is the enzyme–ATP complex, E–A–G is the enzyme–ATP–glutamate complex, E–A–G–N is the enzyme–ATP–glutamate–ammonia complex, and E–P is the γ-glutamyl phosphate intermediate. A standard state of 1 M was used for all substrates.

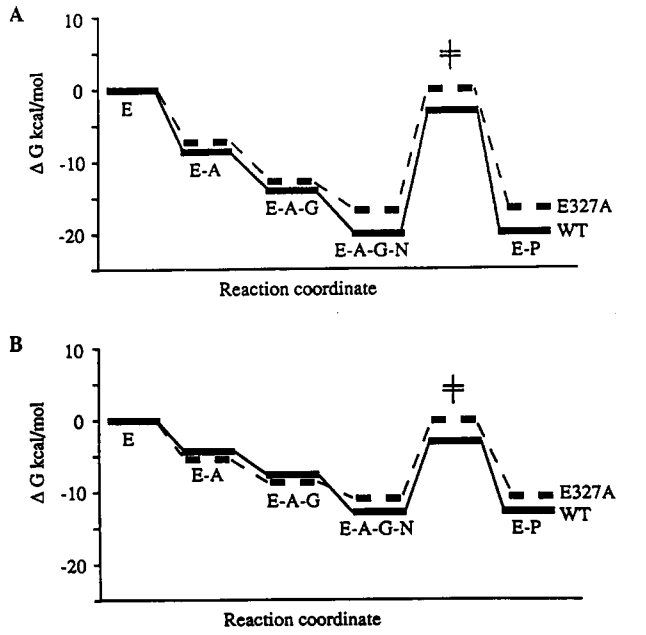

FIGURE 3: Free energy profile for (A) wild-type and E327A Mn^{2+}-activated enzymes and (B) wild-type and E327A Mg^{2+}-activated enzymes. E–A is the enzyme–ATP complex, E–A–G is the enzyme–ATP–glutamate complex, E–A–G–N is the enzyme–ATP–glutamate–ammonia complex, and E–P is the γ-glutamyl phosphate intermediate. A standard state of 1 M was used for all substrates.

transition state for the phosphoryl transfer step. From the results in Table 4, the rate-limiting step is product release (k_5) for the WT and mutant enzymes that contain Mn^{2+}. The D50A-Mn^{2+} enzyme destabilizes both the ground state and transition state for phosphoryl transfer and, hence, does not have a great effect on the catalytic flux of the enzyme (Figure 2). A significant decrease in the K_{int} (k_4/k_{-4}) for phosphoryl transfer (53-fold) is observed upon increasing the length of the carboxyl side chain of Asp-50 in the D50E mutant. This is most likely due to the weaker binding of substrates and destabilization of the γ-glutamyl phosphate intermediate as evidenced by the 66-fold increase in the rate constant for the reverse phosphoryl transfer step (k_{-4}). The E327A-Mn^{2+} enzyme is unable to sufficiently stabilize the ground state and the transition state for phosphoryl transfer compared to the WT-Mn^{2+} enzyme (Figure 3A), and so a substantial amount of catalytic throughput is lost as reflected in the decreased value of the rate constant for the forward phosphoryl transfer reaction (k_3).

Based on the rapid reaction kinetic data, the burst rates observed with Mg^{2+}-activated enzymes at pH 7.5 were fast.

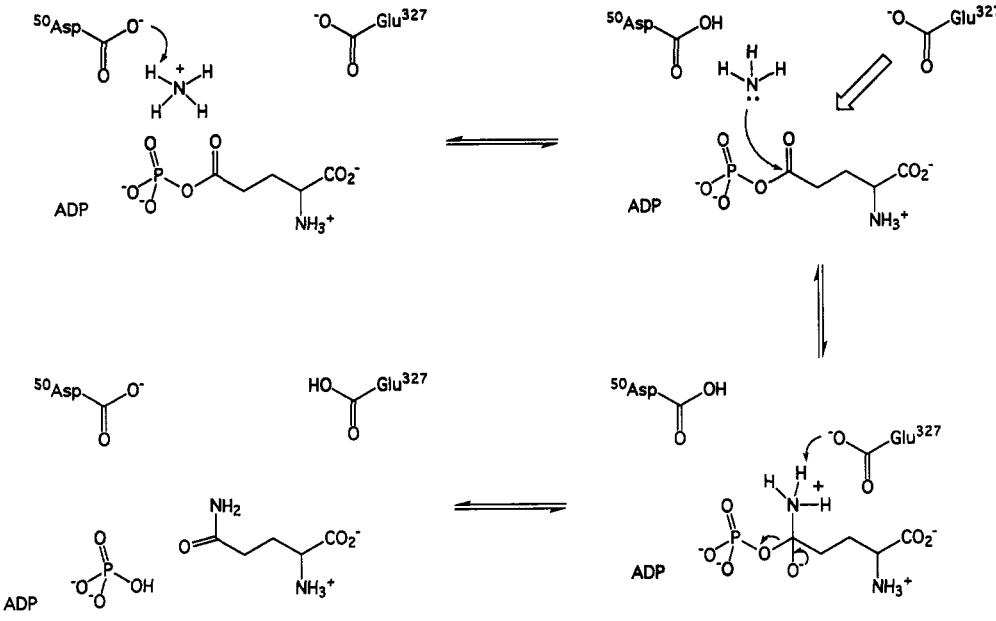

FIGURE 4: Mechanism of glutamine synthetase represented after formation of γ-glutamyl phosphate and binding of NH_4^+. The figure illustrates the role of Asp-50 and Glu-327 residues in catalysis derived from the kinetic data in this paper and the X-ray crystal structure of Liaw and Eisenberg (1993). The large arrow in the top right of the figure represents movement of the Glu-327 loop as revealed in the X-ray structure of the GS complex with methionine sulfoximine, an analog of the tetrahedral adduct depicted at the bottom right in this figure.

Thus, the rate-limiting step for both the wild-type and E327 A Mg^{2+}-activated enzymes was product release. The free energy profiles for the Mg^{2+}-activated wild-type and E327A are shown in Figure 3B. The E327A-Mg^{2+} enzyme has the same effect of destabilizing the ground state of the ternary complex and the transition state for phosphoryl transfer as the Mn^{2+}-activated enzyme. The magnitude of the destabilization in the Mg^{2+}-enzyme is not as great as in the Mn^{2+}-enzyme because of the greater stabilization of the ATP and glutamate complexes in the Mg^{2+}-enzyme. Also, a 4-fold decrease in the internal equilibrium constant for phosphoryl transfer compared to the WT-Mg^{2+} enzyme is observed. This shift in the internal equilibrium constant favoring substrates is due to the 16-fold increase in the rate constant for the reverse phosphoryl transfer compared to the 3.6-fold increase in the rate constant for the forward phosphoryl transfer. All of the data above support the role of Glu-327 in stabilizing formation and/or breakdown of the tetrahedral intermediate as revealed in the X-ray structure (Liaw & Eisenberg, 1994).

Conclusions. The kinetic data reported in this paper support the notion that Asp-50 is involved in binding the substrate NH_4^+ with the additional possibility that Asp-50 is the base that deprotonates NH_4^+ during catalysis. The carboxyl side chain of Glu-327 might incidentally be involved in binding NH_4^+ but definitely has a direct catalytic function in stabilizing the transition state leading to the formation of the γ-glutamyl phosphate intermediate. A model depicting the roles of the residues Asp-50 and Glu-327 in catalysis is illustrated in Figure 4.

REFERENCES

Abell, L. M., & Villafranca, J. J. (1991) *Biochemistry 30*, 1413–1418.

Almassy, R. J., Janson, C. A., Hamlin, R., Xuong, N.-H., & Eisenberg, D. (1986) *Nature 323*, 304–330.

Chen, Y., Backman, K., & Magasanik, B. (1982) *J. Bacteriol. 150*, 214–220.

Clark, D. D., & Villafranca, J. J. (1985) *Biochemistry 24*, 5147–5152.

Colanduoni, J., Nissan, R., & Villafranca, J. J. (1987) *J. Biol. Chem. 262*, 3037–3043.

Denton, M. D., & Ginsburg, A. (1969) *Biochemistry 8*, 1714–1725.

Ginsburg, A., Yeh, J., Hennig, S. B., & Denton, M. D. (1970) *Biochemistry 9*, 633–649.

Hunt, J. B., & Ginsburg, A. (1972) *Biochemistry 11*, 3723–3735.

Hunt, J. B., & Ginsburg, A. (1980) *J. Biol. Chem. 255*, 590–593.

Hunt, J. B., Smyrniotis, P. Z., Ginsburg, A., & Stadtman, E. R. (1975) *Arch. Biochem. Biophys. 166*, 102–124.

Janson, C. A., Kayne, P. S., Almassy, R. J., Grundtein, M., & Eisenberg, D. (1986) *Gene 46*, 297–300.

Johnson, K. A. (1986) *Methods Enzymol. 134*, 677–705.

Johnson, K. A. (1992) in *The Enzymes 20* (3rd ed.) (Sigman, D., & Boyer, P. D., Eds.) pp 1–61.

Liaw, S.-H., & Eisenberg, D. (1994) *Biochemistry* (preceding paper in this issue).

Meek, T. D., Johnson, K. A., & Villafranca, J. J. (1982) *Biochemistry 21*, 2158–2167.

Rhee, S. G., Chock, P. B., & Stadtman, E. R. (1989) *Adv. Enzymol. Relat. Areas Mol. Biol. 62*, 37–92.

Roseman, J. E., & Levine, R. L. (1987) *J. Biol. Chem. 262*, 2101–2110.

Shapiro, B. M., & Ginsburg, A. (1968) *Biochemistry 7*, 2153–2167.

Stadtman, E. R., & Ginsburg, A. (1974) in *The Enzymes 10* (3rd ed.) pp 755–807.

Villafranca, J. J., Ash, D. E., & Wedler, F. C. (1976a) *Biochemistry 15*, 536–543.

Villafranca, J. J., Ash, D. E., & Wedler, F. C. (1976b) *Biochemistry 15*, 544–553.

Villafranca, J. J., Ransom, S. C., & Gibbs, E. J. (1985) *Curr. Top. Cell. Regul. 26*, 207–219.

Wells, T. N. C., & Fersht, A. R. (1986) *Biochemistry 25*, 1881–1886.

Wray, L. V., & Fisher, S. H. (1988) *Gene 71*, 247–256.

Yamashita, M. M., Almassy, R. J., Janson, C. A., Cascio, D., & Eisenberg, D. (1989) *J. Biol. Chem. 264*, 17681–17690.